International Communications in Heat and Mass Transfer 38 (2011) 1019–1023

Contents lists available at ScienceDirect

International Communications in Heat and Mass Transfer

journal homepage: www.elsevier.com/locate/ichmt

Turbulent flow in a composite channel ☆

Renato A. Silva [b], Marcelo J.S. de Lemos [a,*]

[a] *Departamento de Energia — IEME, Instituto Tecnológico de Aeronáutica, ITA, 12228-900, São José dos Campos, SP, Brazil*
[b] *Departamento de Engenharias e Computação, DECOM/CEUNES, Universidade Federal do Espírito Santo, UFES, 29933-415, São Mateus, ES, Brazil*

ARTICLE INFO

Available online 10 May 2011

Keywords:
Clear fluid
Numerical methods
Porous media
Turbulence modeling

ABSTRACT

Numerical solutions for turbulent flow in a composite channel are presented. Here, a channel with a centered porous material is considered. The interface between the porous medium and the clear flow was assumed to have different transversal positions and the porous matrix was simulated with distinct permeabilities. Governing equations were discretized and solved for both domains making use of one unique numerical methodology. Increasing the size of the porous material pushes the flow outwards, increasing the levels of turbulent kinetic energy at the macroscopic interface. For high permeability media, a large amount of mechanical energy is converted into turbulence inside the porous structure.

1. Introduction

Enhancement of thermal efficiency of advanced heat collectors can be achieved by inserting a porous heat sink inside such devices. Accordingly, when modeling porous media, homogenization of local properties is obtained by means of the Volume-Average Theorem (VAT) [1,2]. When the domain presents a macroscopic interfacial area, the literature proposes the existence of a stress jump interface condition between the clear flow region and the porous medium [3,4]. Analytical solutions involving such models have been published [5–7].

Recently, Silva and de Lemos (2003a–b) [8,9] presented numerical solutions for laminar and turbulent flow in a channel partially filled with a flat layer of porous material. There, the authors considered the stress jump condition at the interface. Such works were based on a numerical methodology proposed for hybrid media, *i.e.*, flow systems containing both clear passages and finite porous materials.

It is important to emphasize that the classical problem of having a laminar flow over a finite porous media, inside which a flat low-speed flow occurs, has been studied by Beavers and Joseph (1967) [10]. In that study, neither turbulence in the fluid layer, nor variation of the seepage velocity inside the porous matrix, was considered. Here, both effects are accounted for, or say, turbulence is assumed to exist in the entire domain, including the highly porous material, as well as the axial velocity is made to vary inside the porous structure as the interface is approached. In this sense, the study herein differs substantially from the classical work presented in Beavers and Joseph (1967) [10].

As such, the objective of this paper is to investigate fully developed flow, in turbulent regime, inside a tube containing a highly porous material. In this paper, the size of the porous blockage is varied as well as its permeability. Their effects on the mean and turbulent fields are investigated. Here, only the flow structure is analyzed but extension to heat transfer, including buoyant flows [11] as well as thermal non-equilibrium between the solid and the fluid phase, has also been investigated [12].

2. Macroscopic mathematical model

2.1. Geometry and governing equations

The flow under consideration is schematically shown in Fig. 1 where a channel is partially filled with a layer of a porous material. Constant property fluid flows longitudinally from left to right permeating through both the clear region and the porous structure.

A macroscopic form of the governing equations is obtained by taking the volumetric average of the entire equation set. In this development, the porous medium is considered to be rigid and saturated by the incompressible fluid (see [13] for details).

The macroscopic continuity equation is given by,

$$\nabla \cdot \bar{\mathbf{u}}_D = 0 \qquad (1)$$

where the Dupuit–Forchheimer relationship, $\bar{\mathbf{u}}_D = \phi \langle \bar{\mathbf{u}} \rangle^i$, has been used and $\langle \bar{\mathbf{u}} \rangle^i$ identifies the intrinsic (liquid) average of the local time-

☆ Communicated by W.J. Minkowycz.

* Corresponding author.
E-mail address: delemos@ita.br (M.J.S. de Lemos).

0735-1933/$ – see front matter © 2011 Elsevier Ltd. All rights reserved.
doi:10.1016/j.icheatmasstransfer.2011.04.029

Nomenclature

A_t	Transversal area of channel
c_F	Forchheimer coefficient in Eq. (2)
c's	Constants in Eqs. (5)–(7)
$\mathbf{D}$	Deformation rate tensor, $\mathbf{D}=[\nabla\mathbf{u}+(\nabla\mathbf{u})^T]/2$
Da	Darcy number, $Da=K/(2H)^2$
D_p	Diameter of cylindrical rods
G^i	Production rate of $\langle k\rangle^i$ due to the porous matrix, $G^i=c_k\rho\phi\langle k\rangle^i\lvert\bar{\mathbf{u}}_D\rvert/\sqrt{K}$
$\mathbf{g}$	Gravity acceleration vector
H	Distance between channel walls
h	Thickness of porous layer
h_p	Non-dimensional porous layer thickness, $h_p=h/2H$
$\mathbf{I}$	Unit tensor
k	Turbulent kinetic energy per unit mass, $k=\overline{\mathbf{u}'\cdot\mathbf{u}'}/2$
$\langle k\rangle^v$	Volume (fluid + solid) average of k
$\langle k\rangle^i$	Intrinsic (fluid) average of k
K	Permeability, $K=D_p^2\phi^3/144(1-\phi)^2$
p	Thermodynamic pressure
$\langle p\rangle^i$	Intrinsic (fluid) average of pressure p
P^i	Production rate of k due to mean gradients of $\bar{\mathbf{u}}_D$, $P^i=-\rho\langle\overline{\mathbf{u}'\mathbf{u}'}\rangle^i:\nabla\bar{\mathbf{u}}_D$
$\overline{\mathbf{R}}$	Time average of total drag per unit volume
Re_H	Channel height based Reynolds number, $\mathrm{Re}_H=(\rho\bar{\mathbf{u}}_D 2H)/\mu$
S_ϕ	Source term
$\bar{\mathbf{u}}$	Microscopic time-averaged velocity vector
$\langle\bar{\mathbf{u}}\rangle^i$	Intrinsic (fluid) average of $\bar{\mathbf{u}}$
$\bar{\mathbf{u}}_D$	Darcy velocity vector, $\bar{u}_D=\phi\langle\bar{u}\rangle^i$
$\bar{\mathbf{u}}_{D_i}$	Darcy velocity vector at the interface
$\bar{\mathbf{u}}_{D_p}$	Darcy velocity vector parallel to the interface
$\bar{u}_{D_{in}}$	Average Darcy velocity, $\bar{u}_{D_{in}}=\frac{1}{A_t}\int_{A_t}\bar{u}_D dA$
u_{D_n}, u_{D_p}	Components of Darcy velocity at interface along η (normal) and ξ (parallel) directions, respectively
x, y	Cartesian coordinates

Greek symbols

β	Interface stress jump coefficient
μ	Fluid dynamic viscosity
μ_{eff}	Effective viscosity for a porous medium, $\mu_{eff}=\mu/\varphi$
μ_{t_φ}	Macroscopic turbulent viscosity
ε	Dissipation rate of k, $\varepsilon=\mu\overline{\nabla\mathbf{u}':(\nabla\mathbf{u}')^T}/\rho$
$\langle\varepsilon\rangle^i$	Intrinsic (fluid) average of ε
ρ	Density
ϕ	Porosity
φ	General dependent variable
η, ξ	Generalized coordinates
$\overline{\Delta p}$	Average pressure drop along channel, $\overline{\Delta p}=\frac{1}{A_t}\int_{A_t}(p_{\mathrm{exit}}-p_{\mathrm{inlet}})dA$

Subscripts

t	Turbulent
ϕ	Macroscopic
(s,f)	Solid/fluid

Superscripts

i	Intrinsic (fluid) average
v	Volume (fluid + solid) average

averaged velocity vector $\bar{\mathbf{u}}$ [2,13]. Eq. (1) represents the macroscopic continuity equation for an incompressible fluid in a rigid porous medium.

The macroscopic time-mean Navier–Stokes (NS) equation for an incompressible fluid with constant properties can be written as,

$$\rho\nabla\cdot\left(\frac{\bar{\mathbf{u}}_D\bar{\mathbf{u}}_D}{\phi}\right)=-\nabla\left(\phi\langle\bar{p}\rangle^i\right)+\mu\nabla^2\bar{\mathbf{u}}_D+\nabla\cdot\left(-\rho\phi\langle\overline{\mathbf{u}'\mathbf{u}'}\rangle^i\right)-\left[\frac{\mu\phi}{K}\bar{\mathbf{u}}_D+\frac{c_F\phi\,\rho\,\lvert\bar{\mathbf{u}}_D\rvert\bar{\mathbf{u}}_D}{\sqrt{K}}\right] \tag{2}$$

where μ is the fluid dynamic viscosity, K is the permeability , c_F is known in the literature as the non-linear Forchheimer coefficient and the term $-\rho\phi\langle\overline{\mathbf{u}'\mathbf{u}'}\rangle^i$ is the Macroscopic Reynolds Stress Tensor (MRST). The last two terms in Eq. (2) represent the time-mean total drag per unit volume acting on the fluid by the action of the porous structure [13].

Further, a model for the MRST in analogy with the Boussinesq concept for clear fluid can be written as:

$$-\rho\phi\langle\overline{\mathbf{u}'\mathbf{u}'}\rangle^i=\mu_{t_\phi}2\langle\overline{\mathbf{D}}\rangle^{\mathbf{v}}-\frac{2}{3}\phi\rho\langle k\rangle^i\mathbf{I} \tag{3}$$

where

$$\langle\overline{\mathbf{D}}\rangle^v=\frac{1}{2}\left[\nabla\left(\phi\langle\bar{\mathbf{u}}\rangle^i\right)+\left[\nabla\left(\phi\langle\bar{\mathbf{u}}\rangle^i\right)\right]^T\right] \tag{4}$$

is the macroscopic deformation tensor, $\langle k\rangle^i$ is the intrinsic average for k and μ_{t_ϕ} is the macroscopic turbulent viscosity. The macroscopic turbulent viscosity, μ_{t_ϕ}, used in Eq. (3) is modeled similarly to the case of clear fluid flow and a proposal for it was reviewed in [13] as,

$$\mu_{t_\phi}=\rho\,c_\mu\langle k\rangle^{i^2}/\langle\varepsilon\rangle^i \tag{5}$$

2.2. Macroscopic equations for k and ε

Transport equations for $\langle k\rangle^i=\langle\overline{\mathbf{u}'\cdot\mathbf{u}'}\rangle^i/2$ and $\langle\varepsilon\rangle^i=\mu\langle\overline{\nabla\mathbf{u}':(\nabla\mathbf{u}')^T}\rangle^i/\rho$ in their so-called High Reynolds Number form are reviewed by de Lemos (2006) [13] as:

$$\rho\nabla\cdot\left(\bar{\mathbf{u}}_D\langle k\rangle^i\right)=\nabla\cdot\left[\left(\mu+\frac{\mu_{t_\phi}}{\sigma_k}\right)\nabla\left(\phi\langle k\rangle^i\right)\right]+P^i+G^i-\rho\phi\langle\varepsilon\rangle^i \tag{6}$$

$$\rho\nabla.\left(\bar{\mathbf{u}}_D\langle\varepsilon\rangle^i\right)=\nabla\cdot\left[\left(\mu+\frac{\mu_{t_\phi}}{\sigma_\varepsilon}\right)\nabla\left(\phi\langle\varepsilon\rangle^i\right)\right]+c_1P^i\frac{\langle\varepsilon\rangle^i}{\langle k\rangle^i}+c_2\frac{\langle\varepsilon\rangle^i}{\langle k\rangle^i}\left(G^i-\rho\phi\langle\varepsilon\rangle^i\right) \tag{7}$$

where the c's are constants, $P^i=-\rho\langle\overline{\mathbf{u}'\mathbf{u}'}\rangle^i:\nabla\bar{\mathbf{u}}_D$ is the production rate of $\langle k\rangle^i$ due to gradients of $\bar{u}_D$ and $G^i=c_k\rho\phi\langle k\rangle^i\lvert\bar{\mathbf{u}}_D\rvert/\sqrt{K}$ is the generation rate of the intrinsic average of k due to the action of the porous matrix.

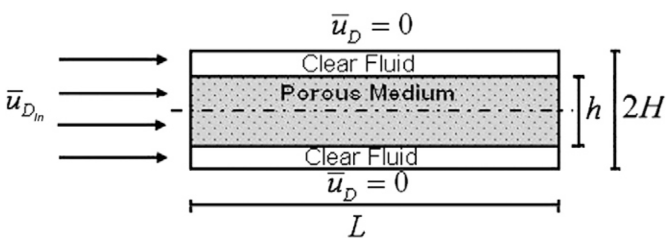

Fig. 1. Channel with porous layer.

2.3. Interface conditions

The equation proposed by Ochoa–Tapia and Whitaker (1995a–b) [3,4] for describing the stress jump at the interface between the clear flow region and the porous structure is given by,

$$\mu_{eff}\frac{\partial u_{D_p}}{\partial \eta}\bigg|_{\text{Porous Medium}} - \mu\frac{\partial u_{D_p}}{\partial \eta}\bigg|_{\text{Clear Fluid}} = \beta\frac{\mu}{\sqrt{K}}u_{D_p}\bigg|_{\text{interface}} \qquad (8)$$

where u_{D_p} is the Darcy velocity component parallel to the interface, μ_{eff} is the effective viscosity for the porous region, and β an adjustable coefficient that accounts for the stress jump at the interface. Here, for simplicity, no such stress jump is considered ($\beta=0$).

In addition to Eq. (8), continuity of velocity, fluid pressure, statistical variables and their fluxes across the interface are given by,

$$\bar{\mathbf{u}}_D\big|_{\text{Porous Medium}} = \bar{\mathbf{u}}_D\big|_{\text{Clear Fluid}} \qquad (9)$$

$$\langle\bar{p}\rangle^i\big|_{\text{Porous Medium}} = \langle\bar{p}\rangle^i\big|_{\text{Clear Fluid}} \qquad (10)$$

$$\langle k\rangle^v\big|_{\text{Porous Medium}} = \langle k\rangle^v\big|_{\text{Clear Fluid}} \qquad (11)$$

$$\left(\mu + \frac{\mu_{t_\varphi}}{\sigma_k}\right)\frac{\partial\langle k\rangle^v}{\partial y}\bigg|_{\text{Porous Medium}} = \left(\mu + \frac{\mu_t}{\sigma_k}\right)\frac{\partial\langle k\rangle^v}{\partial y}\bigg|_{\text{Clear Fluid}} \qquad (12)$$

$$\langle\varepsilon\rangle^v\big|_{\text{Porous Medium}} = \langle\varepsilon\rangle^v\big|_{\text{Clear Fluid}} \qquad (13)$$

$$\left(\mu + \frac{\mu_{t_\varphi}}{\sigma_\varepsilon}\right)\frac{\partial\langle\varepsilon\rangle^v}{\partial y}\bigg|_{\text{Porous Medium}} = \left(\mu + \frac{\mu_t}{\sigma_\varepsilon}\right)\frac{\partial\langle\varepsilon\rangle^v}{\partial y}\bigg|_{\text{Clear Fluid}} \qquad (14)$$

Further, the extension of Eq. (8) to the case of turbulent flow can be given as,

$$\left(\mu_{eff} + \mu_{t_\varphi}\right)\frac{\partial\bar{u}_{D_p}}{\partial y}\bigg|_{\text{Porous Medium}} - (\mu + \mu_t)\frac{\partial\bar{u}_{D_p}}{\partial y}\bigg|_{\text{Clear Fluid}} = (\mu + \mu_t)\frac{\beta}{\sqrt{K}}\bar{u}_{D_p}\bigg|_{\text{interface}} \qquad (15)$$

Eqs. (9) and (10) were also proposed by Ochoa–Tapia and Whitaker (1995a) [3] whereas relationships Eqs. (11) through (15) were used by Lee and Howell (1987) [14].

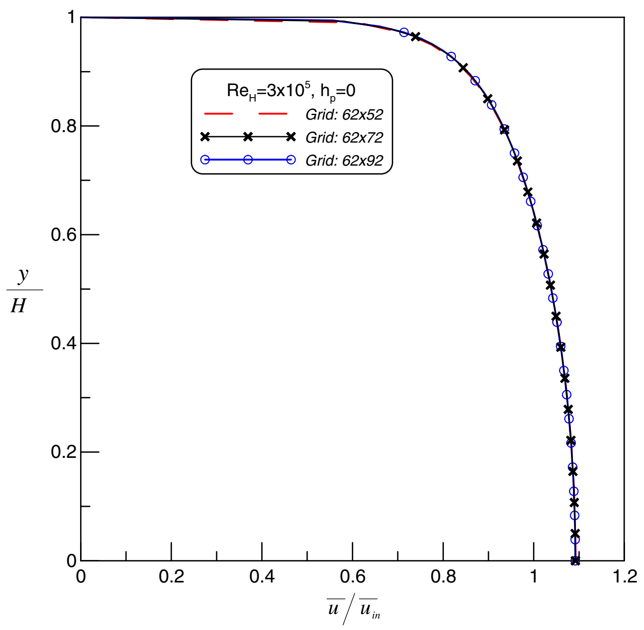

Fig. 2. Effect of grid size on velocity field.

3. Numerical details

In Silva and de Lemos (2003a) [8], the discretization methodology used for including the jump condition in the numerical solutions was discussed in detail. For that, only brief comments about the numerical procedure are here made. Transport equations are discretized in a generalized coordinate system η–ξ using the control volume method. The faces of the volume are formed by lines of constant coordinates η–ξ.

The use of the spatially periodic boundary condition along the x coordinate was also discussed in Silva and de Lemos (2003a–b) [8,9] and was applied in order to simulate fully developed flow. The spatially periodic condition was implemented by running the 2D

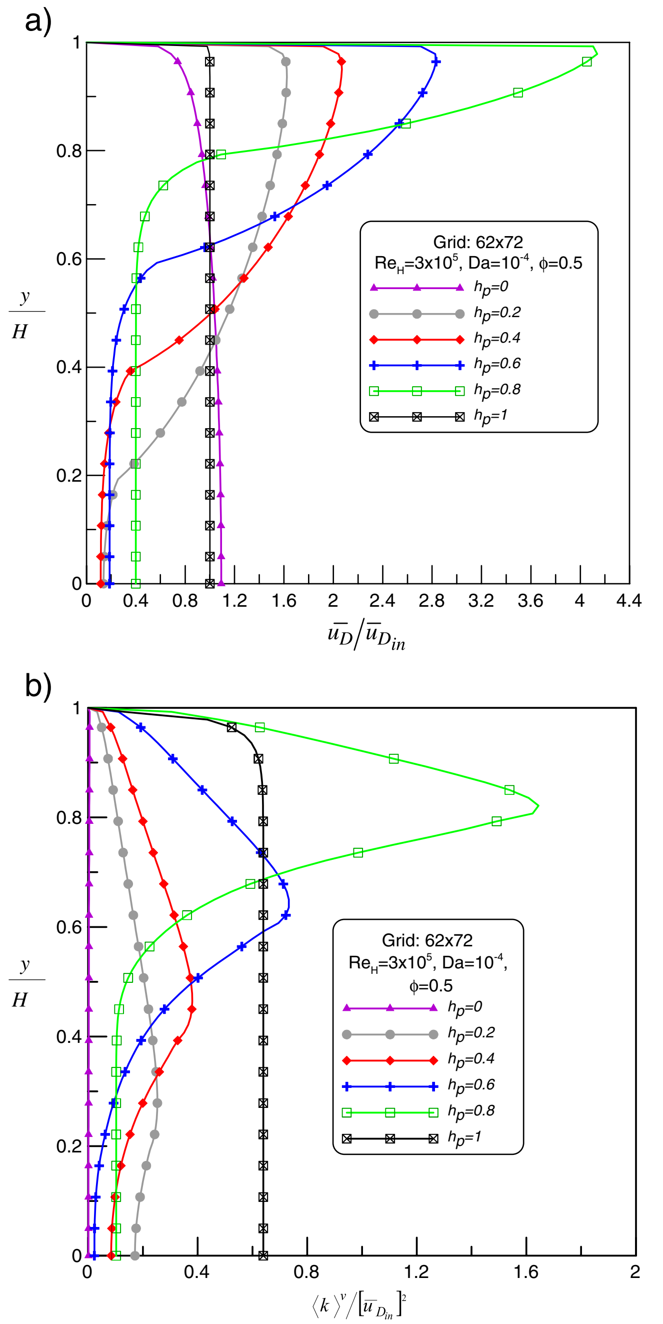

Fig. 3. Effect of porous layer thickness $h_p=h/H$ (see Fig. 1): a) non-dimensional mean velocity, b) non-dimensional turbulent kinetic energy.

solution repetitively, until outlet profiles in $x=L$ matched those at the inlet ($x=0$).

For steady-state condition, the standard form of the discrete equations for a general variable φ becomes [15],

$$I_e + I_w + I_n + I_s = S_\phi \tag{16}$$

where I_e, I_w, I_n e I_s are the fluxes of φ at *east*, *west*, *north* and *south* faces of the control volume and S_φ is a source term. All computations were carried out until normalized residues of the algebraic equations were brought down to 10^{-7}. As also explained in Silva and de Lemos (2003a) [8], the interface was positioned dividing two control volumes, one being entirely located in the porous region and the other lying in the clear fluid. The computational grid based on the generalized coordinate system η–ξ is such that the macroscopic interface coincides with a line of constant η, extending itself along the ξ coordinate. In this arrangement, the face connecting two neighbor volumes, each one located on each side of the macroscopic interface, belongs to the macroscopic interface between the two media. With that, $\bar{u}_{D_i}$ is the Darcy velocity at the interface and $\bar{u}_{D_p}$ stands for its parallel component. Details of the discretization of the terms on the left and right of Eq. (15) can be found in Silva and de Lemos (2003a) [8].

4. Results and discussion

The flow in Fig. 1 was computed with the set of Eqs. (2)–(7) including constitutive Eq. (3) and the Kolmogorov–Prandtl expression Eq. (5). The wall function approach was used for treating the flow close to the walls. Simulation of the fully developed condition required the use of the spatially periodic condition, as already mentioned.

Grid independence studies are presented in Fig. 2. The figure shows several non-dimensional velocity profiles for $h_p=0$ (clear channel) and Reynolds number $Re_H=3\times10^5$. One should note that here the definition of Re_H for a two-dimensional channel of height $2H$ is given by $Re_H = (\rho\bar{\mathbf{u}}_D 2H)/\mu$. The curves in Fig. 2 indicate that for more than 72 nodal points in the cross-stream direction, the solution is essentially grid independent. Further, one should recall that the numerical methodology here considered was focused on two dimensional flows, so that simulating fully developed cases shown in the figures required the used of nodal points along the axial direction and the employment of the spatially periodic condition mentioned earlier. For all runs here studied, a total of 62 nodes in the axial direction was found to suffice.

The effect of h_p is shown next in Fig. 3. The mean velocity in Fig. 3a shows that as the size of the porous material increases, the fluid is pushed outwards and forced to flow in the clear passage, increasing the velocity gradient at the wall. Consequently, enhanced heat transfer rates are expected to exist for larger porous blockages. Fig. 3b shows corresponding profiles for the non-dimensional turbulent kinetic energy defined as $\langle k\rangle^v/(\bar{u}_{D_{in}})^2$. As the interface approaches, most of the kinetic energy is produced around it, whose peak increases as the free flow gap is reduced. However, the larger the blockage size, the larger the necessary pressure drop to pump the flow though the tube (Fig. 4), a result that must be taken into consideration

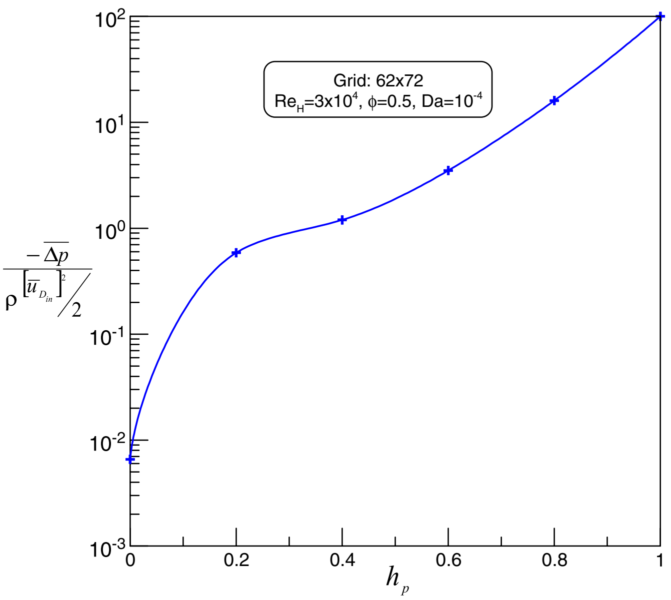

Fig. 4. Pressure drop as a function of porous layer thickness h_p.

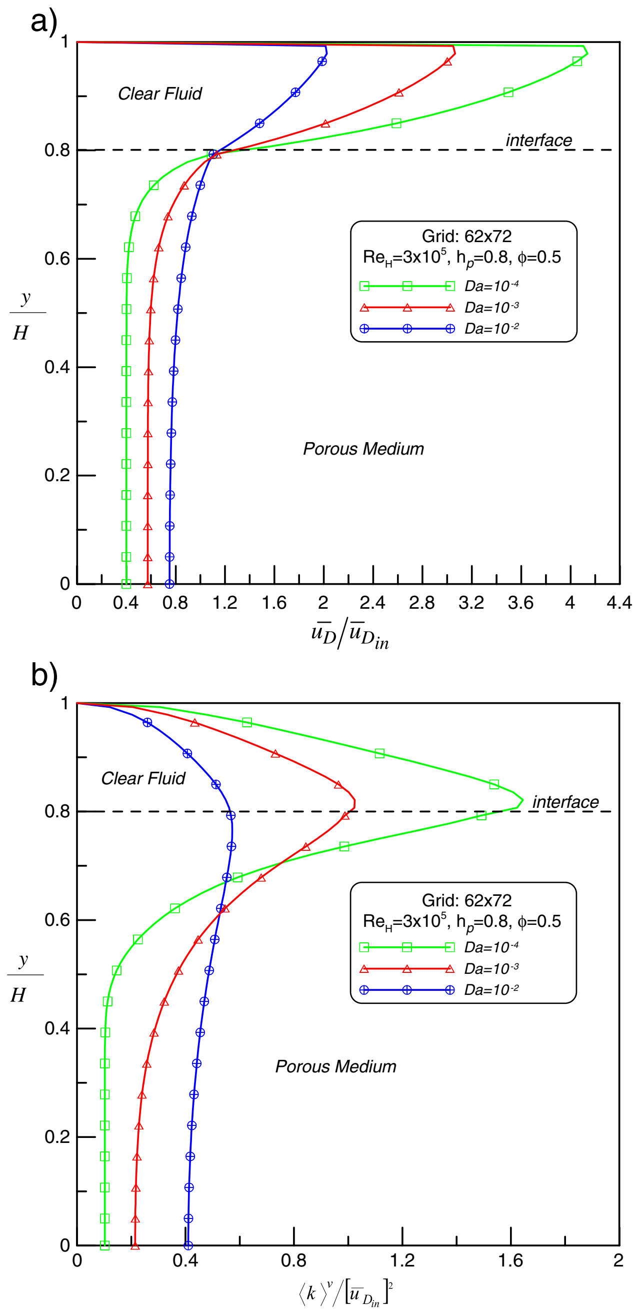

Fig. 5. Effect of Da on: a) mean velocity, b) turbulent kinetic energy.

when considering heat systems involving channels with porous material inside.

Fig. 5 finally shows the effect of Darcy number on the fluid structure. As the porous material becomes more permeable, less fluid flows though the clearance between the wall and the interface (Fig. 5a). Corresponding profiles for $\langle k \rangle^v/(\bar{u}_{D_{in}})^2$ are presented in Fig. 5b and shows that for low permeability cases, the flow tend towards an annular flow, with the peak of k located around the interface. On the other hand, as the fluid permeates the porous matrix more easily, most of the turbulent kinetic energy is generated inside the porous medium, indicating that mean mechanical energy of the flow is transformed into turbulence, a flow feature modeled by the extra generation term G^i in Eq. (6).

5. Conclusions

Numerical solutions for turbulent flow in a composite channel were obtained. The interface between the porous medium and the clear flow was assumed to have different radial positions and the porous matrix was simulated with distinct permeabilities. Governing equations were discretized and solved for both domains making use of one unique numerical methodology. Increasing the size of the porous material pushes the flow outwards, increasing the levels of turbulent kinetic energy at the macroscopic interface. For high permeability media, a large amount of mechanical energy is converted into turbulence inside the porous structure.

Acknowledgments

The authors would like to thank CNPq and FAPES, Brazil, for their invaluable financial support during the preparation of this work.

References

[1] S. Whitaker, Advances in theory of fluid motion in porous media, Industrial & Engineering Chemistry 61 (12) (1969) 14–28.
[2] W.G. Gray, P.C.Y. Lee, On the theorems for local volume averaging of multiphase system, International Journal of Multiphase Flow 3 (4) (1977) 333–340.
[3] J.A. Ochoa-Tapia, S. Whitaker, Momentum transfer at the boundary between a porous medium and a homogeneous fluid – I. Theoretical development, International Journal of Heat and Mass Transfer 38 (14) (1995) 2635–2646.
[4] J.A. Ochoa-Tapia, S. Whitaker, Momentum transfer at the boundary between a porous medium and a homogeneous fluid – II. Comparison with experiment, International Journal of Heat and Mass Transfer 38 (14) (1995) 2647–2655.
[5] A.V. Kuznetsov, Analytical investigation of the fluid flow in the interface region between a porous medium and a clear fluid in channels partially filled with a porous medium, Applied Scientific Research 56 (1) (1996) 53–67.
[6] A.V. Kuznetsov, Influence of the stress jump condition at the porous-medium/clear-fluid interface on a flow at a porous wall, International Communications in Heat and Mass Transfer 24 (3) (1997) 401–410.
[7] A.V. Kuznetsov, Fluid mechanics and heat transfer in the interface region between a porous medium and a fluid layer: a boundary layer solution, Journal of Porous Media 2 (3) (1999) 309–321.
[8] R.A. Silva, M.J.S. de Lemos, Numerical analysis of the stress jump interface condition for laminar flow over a porous layer, Numerical Heat Transfer – Part A Applications 43 (6) (2003) 603–617.
[9] R.A. Silva, M.J.S. de Lemos, Turbulent flow in a channel occupied by a porous layer considering the stress jump at the interface, International Journal of Heat and Mass Transfer 46 (26) (2003) 5113–5121.
[10] G.S. Beavers, D.D. Joseph, Boundary conditions at a naturally permeable wall, Journal of Fluid Mechanics 30 (1) (1967) 197–207.
[11] E.J. Braga, M.J.S. de Lemos, Laminar natural convection in cavities filled with circular and square rods, International Communications in Heat and Mass Transfer 32 (10) (2005) 1289–1297.
[12] M.B. Saito, de Lemos, Interfacial heat transfer coefficient for non-equilibrium convective transport in porous media, International Communications in Heat and Mass Transfer 32 (5) (2005) 666–676 2005.
[13] M.J.S. de Lemos, Turbulence in porous media: modeling and applications, Elsevier, Kidlington, 2006.
[14] K. Lee, J.R. Howell, Forced convective and radiative transfer within a highly porous layer exposed to a turbulent external flow field, Proceedings of the 1987 ASME-JSME Thermal Engineering Joint Conf., 2, 1987, pp. 377–386.
[15] S.V. Patankar, Numerical heat transfer and fluid flow, Hemisphere, New York, 1980.